Ecology, 101(6), 2020, e03011

Parameterized maximum entropy models predict variability of metabolic scaling across tree communities and populations

Meng Xu [1]

Department of Mathematics, Pace University, 41 Park Row, New York, New York 10038 USA

Citation: Xu, M. 2020. Parameterized maximum entropy models predict variability of metabolic scaling across tree communities and populations. Ecology 101(6):e03011. 10.1002/ecy.3011

Abstract. The maximum entropy theory of ecology (METE) applies the concept of "entropy" from information theory to predict macroecological patterns. The energetic predictions of the METE rely on predetermined metabolic scaling from external theories, and this reliance diminishes the testability of the theory. In this work, I build parameterized METE models by treating the metabolic scaling exponent as a free parameter, and I use the maximum-likelihood method to obtain empirically plausible estimates of the exponent. I test the models using the individual tree data from an oak-dominated deciduous forest in the northeastern United States and from a tropical forest in central Panama. My analysis shows that the metabolic scaling exponents predicted from the parameterized METE models deviate from that of the metabolic theory of ecology and exhibit large variation, at both community and population levels. Assemblage and population abundance may act as ecological constraints that regulate the individual-level metabolic scaling behavior. This study provides a novel example of the use of the parameterized METE models to reveal the biological processes of individual organisms. The implication and possible extensions of the parameterized METE models are discussed.

Key words: constraint-based modeling; individual size distribution; Kolmogorov-Smirnov test; Lagrange multipliers; maximum likelihood; metabolic energy rate; mixed-effects models; phenomenological models.

Introduction

The maximum entropy theory of ecology (METE; Harte et al. 2008, 2009, Harte 2011, Harte and Newman 2014) was developed from information theory and the entropy concept of thermodynamics (Shannon 1948, Jaynes 1957). The METE has been used to model various ecological scaling patterns and relationships, including the species–area relationship (McGlinn et al. 2013, Harte and Kitzes 2015), species abundance distribution (White et al. 2012, Xiao et al. 2015), and individual metabolic rate distributions for species populations and communities (Newman et al. 2014, Xiao et al. 2015). The model's success in predicting a wide range of ecological patterns, the parsimony in its formulations, and its applicability to various taxa across habitats and scales make METE a unified theory in ecology (McGill 2010, Harte 2011, Harte and Newman 2014).

The general principle of the METE is to maximize the information entropy (which reflects our ignorance about a studied system) given a set of constraints representing our prior knowledge about the system. Specifically, the information entropy is maximized with respect to the function of two probability distributions: one is the joint conditional probability of the abundance of a species and the metabolic energy rate of an individual of any species with the same abundance, and the other is the conditional probability of the spatial abundance of each species (Harte 2011, Bertram 2015, Favretti 2017, Brummer and Newman 2019). These probability distributions are conditioned on four state variables of the living system: total area (A_0), number of species (S_0), total number of individuals (N_0), and total rate of metabolic energy (E_0). Unlike process-based theories (e.g., the unified neutral theory; see Hubbell 2001), predictions of the METE are not derived from specific biological mechanisms, but rather from macroscopic characteristics of the studied system. Such characteristics are represented as constraint equations that use the state variables, making METE a constraint-based theory. Energetic predictions of the METE rely on the metabolic scaling predicted from other theories (Harte 2011).

Metabolic rate is one of the fundamental metrics in ecology and evolution, as it holds key information on an individual's growth and energy use (Steyermark 2002, Sears 2005, Biro and Stamps 2010, Rosenfeld et al. 2015), and it has profound implications for the stability and diversity of ecological populations and communities (Brown et al. 2004, Savage et al. 2004*a*). Empirical evidence shows that the bivariate relationship between metabolic rate and individual body size follows a power function (White and Seymour 2003, 2005, Reich et al. 2006), although the exact value of the power exponent

Manuscript received 8 July 2019; revised 7 November 2019; accepted 3 January 2020; final version received 13 February 2020. Corresponding Editor: Bruce E. Kendall.
[1]E-mail: mxu@pace.edu

(*b*) remains controversial (Dodds et al. 2001, White et al. 2007*a*, *b*). Previous studies on universal metabolic scaling used body mass as the proxy for individual size and pinpointed *b* as mostly either 2/3 (Huxley 1932, Heusner 1982, Bennett and Harvey 1987) or 3/4 (Kleiber 1932, Hemmingsen 1960). Others have found empirical evidence that *b* is heterogeneous across biological taxa and ecological conditions (Bokma 2004, Glazier 2005, Sieg et al. 2009, Isaac and Carbone 2010). On the other hand, numerous models have been proposed to explain the specific values of *b* but have generated conflicting results (Agutter and Wheatley 2004). For example, Rubner (1883) explained the 2/3 power-law scaling between the metabolic rate and body mass by using the surface-area-to-volume ratio of organisms for heat production. West et al. (1997) constructed a fractal branching network model for resource flow that predicted *b* as being 3/4, which is one of the many predictions of the metabolic theory of ecology (West et al. 1999). For vascular plants, the metabolic theory of ecology also predicts that the body mass scales as a power function of the branch diameter with an exponent of 8/3. This implies that $b = 2$ in the scaling relationship between metabolic rate and diameter (metabolic rate $\propto$ mass$^{3/4}$ $\propto$ (diameter$^{8/3}$)$^{3/4}$ $\propto$ diameter^2; where $\propto$ means "is proportional to") (Muller-Landau et al. 2006).

The empirical variability and the theoretical universality of *b* reflect a long-standing disconnect between the testing and modeling of metabolic scaling patterns, which I call the downscaling–upscaling dilemma. Traditionally, empirical tests of metabolic scaling are performed using interspecific compilations of records of metabolic rate and body mass (Nagy et al. 1999, White et al. 2007*a*, *b*, Sieg et al. 2009), which often ignore individual variation and are convoluted with other patterns (e.g., the abundance–size relationship) to infer general rules in ecology (e.g., the energetic equivalence rule; Damuth 1981, Allen et al. 2002, Russo et al. 2003). On the other hand, the majority of metabolic scaling models are based on the physical laws of the internal architecture and physiology of organisms (Patterson 1992, West et al. 1999, Agutter and Wheatley 2004), which neglect ecological or environmental variables that may act as constraints on living organisms (Glazier 2010). Resolution of the discrepancy in the empirical and theoretical values of *b* requires building a unified framework for the testing and modeling of metabolic scaling at the same biological level.

This work aims to build an integrated model of metabolic scaling using the METE and empirical data. Particularly, I modify the METE by introducing *b* as a free parameter in the model, without borrowing hypothetical values from external theories (Harte 2011, Rominger and Merow 2017). Then, I take advantage of the METE probabilistic predictions of individual size distribution and construct-associated likelihood functions. I define individual size distribution as the probability density of rescaled body sizes of the individuals (body sizes divided by the smallest body size) from a community or a population (Harte 2011, Newman et al. 2014; also called the individual power distribution by Rominger and Merow 2017 and Harte et al. 2017). Finally, I use the likelihood functions and individual size data to obtain the maximum-likelihood estimates of *b*. My parameterized METE models allow empirically plausible estimation (i.e., maximum-likelihood method) of the metabolic scaling exponent, standard evaluation and comparison of model performance (e.g., Akaike information criterion), and direct interpretation of the effects of modeling variables (e.g., N_0 and S_0) on *b*. I test the parameterized METE models against the rescaled diameter at breast height data (as a proxy for body size) for individual trees from a deciduous temperate forest in the northeastern United States and from a tropical moist forest in central Panama.

Methods

Data

Black Rock Forest is a deciduous temperate forest located in Cornwall, New York, USA. The study area consists of 12 contiguous plots (each of 75 m by 75 m, or approximately 0.56 ha) located at the north slope site of the forest (see Cohen et al. 2012:fig 7 for the site map). Each plot is subdivided into nine square subplots of equal area (each of 25 m by 25 m, or approximately 0.06 ha), with each subplot denoted by its relative geographical location in the plot (e.g., SW represents the subplot situated in the southwest corner of the plot). During July and August of 2007, within each plot, all oak trees with a diameter at breast height (dbh) of at least 2.4 cm were identified to species and measured. Within each central subplot of a plot, all non-oak trees with a dbh of at least 2.4 cm were identified to species and measured. The total area of the 12 plots (where all oaks were recorded) is approximately 6.14 ha and the total area of the 12 central subplots (where all trees were recorded) is approximately 0.83 ha. Prior to 2007, no major human disturbance had occurred in the study area dating back to the 1930s. In total, 2026 individual trees were recorded in the data (Schuster 2007). I did not use 45 records of dead or small trees (dbh < 2.4 cm), leaving 1,317 live oaks and 664 live non-oaks for analysis. The remaining 1,981 (= 1,317 + 664) trees belonged to 25 species (five oak species and 20 non-oak species), of which 9 species each had at least 10 individuals (with common names, codes, and numbers of individuals in parentheses): *Quercus rubra* (red oak, RO, 782), *Quercus prinus* (chestnut oak, CO, 403), *Acer rubrum* (red maple, RM, 193), *Nyssa sylvatica* (black gum, BG, 148), *Betula lenta* (black birch, BB, 135), *Acer saccharum* (sugar maple, SM, 102), *Quercus alba* (white oak, WO, 69), *Quercus velutina* (black oak, BO, 61), and *Fagus grandifolia* (American beech, BE, 41). These nine species represent most of the trees (97.6% $\approx$ 1,934/1,981) in the

analyzed data. A complete list of the 25 species (including species codes and scientific and common names) is given in Appendix S1: Table S1.

Diameter data of individual trees were also obtained from the 50-hectare plot (1,000 m by 500 m) on the Barro Colorado Island in central Panama (Condit 1998, Hubbell et al. 1999, Hubbell et al. 2005). The whole plot can be subdivided into 1,250 quadrats (each 20 m by 20 m, or 0.04 ha). Between 1982 and 2015, eight censuses were conducted to identify and measure every woody plant (excluding lianas) with a dbh of at least 10 mm in the plot. A tree is defined as an individual stem of at least 10-mm dbh. The dbh data of individual live trees from the most recent census in 2015 were used for analysis. In 2015, the total number of live trees was 248,835, and these trees belonged to 296 species. The complete census data and all species names are publicly available (Condit et al. 2019*a*, *b*). The five species (with their species codes and numbers of individuals in parentheses) with the most individuals were *Hybanthus prunifolius* (HYPR; 37,123), *Faramea occidentalis* (FAOC; 26,420), *Desmopsis panamensis* (DEPA; 13,048), *Trichilia tuberculate* (TRTU; 11,779), and *Alseis blackiana* (ALBL; 8,701). At least 100 individuals were present for each of 160 species. These 160 species represented 98.4% (≈ 244,817/248,835) of all the live trees.

I tested the parameterized METE models using the individual tree dbh data from the Black Rock Forest in 2007 and from the Barro Colorado Island in 2015. These data sets present two forest habitats and environments (a temperate deciduous forest in the Black Rock Forest and a tropical moist forest on the Barro Colorado Island), with contrasting species richness (25 species in the Black Rock Forest plots and 296 species in the Barro Colorado Island plot) and plant density (323 individuals per hectare in the Black Rock Forest plots and 4,977 individuals per hectare in the Barro Colorado Island plot). These differences allow an examination of the robustness of the parameterized METE models for empirical analyses. In addition, the spatial hierarchical structure of the Black Rock Forest data (12 plots and 12 central subplots) will be used to study the effect of spatial scale on the predicted metabolic scaling exponent. Similar spatial hierarchy can be designed for the Barro Colorado Island data, but will not be analyzed here.

Parameterized METE models for individual size distribution

The maximum entropy theory of ecology (METE) makes explicit predictions for the distribution of rescaled metabolic rates (metabolic rates divided by the smallest metabolic rate, denoted by ε) of all individuals in a community or in a conspecific population. At the community level, METE predicts that the distribution of the rescaled metabolic rates of all individuals within a community (denoted as $\Psi(\varepsilon)$) is approximately as follows:

$$\Psi(\varepsilon) \approx \frac{\lambda_2 e^{-\gamma}\left[\frac{1-(N_0+1)e^{-N_0\gamma}+N_0e^{-(N_0+1)\gamma}}{(1-e^{-\gamma})^2}\right]}{e^{-\beta}\left(\frac{1-e^{-\beta N_0}}{1-e^{-\beta}}\right)} \quad (1)$$

where N_0 is the total number of individuals in the community. $\beta = \lambda_1 + \lambda_2$, $\gamma = \lambda_1 + \lambda_2\varepsilon$, and $\sigma = \lambda_1 + \lambda_2 E_0$, with E_0 being the total rescaled metabolic rates of the community $\left(\sum_{i=1}^{N_0}\varepsilon_i\right)$, and with λ_1 and λ_2 being the Lagrange multipliers from the constraint equations of METE (Harte 2011:Eqs. 7.19 and 7.20 or Eqs. S4 and S5 in Appendix S1). λ_1, λ_2, and β are community-level constants that do not vary among species or individuals, whereas ε and, thus, γ are individual-level variables. At the population level, for a species with a given number of individuals (say n), the METE predicts the intraspecific distribution of the rescaled metabolic rate (denoted as $\Theta(\varepsilon|n)$) as follows:

$$\Theta(\varepsilon|n) \approx n\lambda_2 e^{-\lambda_2 n(\varepsilon-1)}. \quad (2)$$

here λ_2 is as defined in Eq. 1.

In practice, testing Eqs. 1 and 2 empirically is impossible, unless the measurement for the individual metabolic rate is available. Previous works of METE (Harte 2011, Newman et al. 2014, Xiao et al. 2015) resolved this problem by converting individual size (often easily measurable) to metabolic rate through allometric scaling theories. For example, the metabolic theory of ecology predicts that metabolic rate $\propto$ mass$^{3/4}$ $\propto$ dbh^2 for individual tree stems (West et al. 1999; see Introduction). In the original formulation of the METE (Eqs. 1 and 2), the power of the rescaled individual size is used as a surrogate for the rescaled metabolic rate following the metabolic theory of ecology (i.e., $\varepsilon = (\text{dbh}/\min(\text{dbh}))^2 = d^2$, where min(dbh) is the smallest dbh, and d is the rescaled dbh of all individuals within the studied system) (Brummer and Newman 2019). In addition, because the METE borrows the metabolic scaling exponent predicted by the metabolic theory of ecology, the assumption used to make the prediction by the metabolic theory of ecology is also required by the METE. That is, variables related to the scaling coefficient (e.g., temperature and activation energy) are invariant among individuals within the studied system.

In this work, I make a novel modification of the original METE by treating the metabolic scaling exponent (b) as a free parameter in the METE predictions, so that, for each individual, the rescaled metabolic rate is equal to a power of the rescaled dbh ($\varepsilon = d^b$), where b is an unknown constant for a community or population. This change allows me to transform the METE predictions of rescaled metabolic rate distribution to probabilistic models and compare them with other phenomenological models (Muller-Landau et al. 2006) at an equal footing (i.e., using likelihood functions). More importantly, it permits empirically meaningful estimations of b. Consequently, the total rescaled metabolic rate within a

community (E_0) is not a constant, as assumed in the original METE formulations, but instead is a function of b $\left(E_0 = \sum_{i=1}^{N_0} (d_i)^b\right)$, where d_i is the rescaled dbh of the ith individual in a community with N_0 individuals). I transform the rescaled metabolic rate distribution (Eqs. 1 and 2) to the individual size distribution (ISD; of rescaled dbh, denoted as d; see Introduction) using the change-of-variable formula (see Harte 2011:box 3.2). METE parameterized as such predicts the ISD of all individuals within a community as follows:

$$\Xi(d) := \frac{\partial \varepsilon}{\partial d} \cdot \Psi(d^b) \approx b \cdot d^{b-1} \cdot \frac{\lambda_2 e^{-\gamma(d)} \left[\frac{1-(N_0+1)e^{-N_0\gamma(d)}+N_0 e^{-(N_0+1)\gamma(d)}}{(1-e^{-\gamma(d)})^2}\right]}{e^{-\beta}\left(\frac{1-e^{-\beta N_0}}{1-e^{-\beta}}\right)} \quad (3)$$

and the ISD of conspecifics within a population is predicted as follows:

$$\rho(d) := \frac{\partial \varepsilon}{\partial d} \cdot \Theta\left(d^b | n\right) \approx b \cdot d^{b-1} \cdot n\lambda_2 e^{-\lambda_2 n\left(d^b - 1\right)}. \quad (4)$$

I design the data analysis of these parameterized METE models (Eqs. 3 and 4) in the following section and present their mathematical details in Appendix S1.

Data analysis

I analyzed the tree data and the parameterized METE models (Eqs. 3 and 4) at two ecological resolutions: community and population.

For the Black Rock Forest data, I defined a tree community as the collection of all trees (regardless of species) within each central subplot of a plot, where all trees were measured. This yielded 12 spatially separate (central subplot) communities for analysis. In addition, within each plot (for oak species) or each central subplot (for non-oak species), I defined a tree population as the collection of all trees of a single species with at least 10 individuals. I did not combine the same species from different plots for the population-level analysis, which relied on community-level constants (λ_1 and λ_2) derived from spatially separate central subplots. In total, 47 species populations (each with a unique plot–species pair, where plot means the species was surveyed either in the plot or in the central subplot within the corresponding plot) were analyzed. Individuals' dbh measurements were rescaled (see Parameterized METE models for individual size distribution) so that the smallest rescaled dbh (d) and the smallest rescaled metabolic rate (ε) for a given population or community were always one.

For the Barro Colorado Island data, I defined a tree community as the collection of all trees (regardless of species) within the entire 50-ha plot or within each 0.04-ha quadrat of the plot separately. I defined a tree population as the collection of all trees of a single species with at least 100 individuals in the entire plot, which resulted in 160 species populations for analysis. The individual dbh measurements were rescaled as explained in the previous section.

For each tree community, I first calculated the community-level constant β using a simplified nonlinear constraint equation from the METE (Harte 2011: Eq. 7.27, or Eq. S6 in the Appendix S1). I then substituted the solution for β into Eq. 3 through $\lambda_1 = \beta - \lambda_2$ and $\lambda_2 \approx S_0/(E_0 - N_0) = S_0/(\sum_{i=1}^{N_0} d_i^b - N_0)$ (see Harte 2011: Eq. 7.26, or from Eqs. S8 and S9 in Appendix S1, where S_0 is the number of distinct species in a community). The likelihood function for the community-level ISD was defined as the product of its density function (Eq. 3) at the rescaled dbh values (assuming independence among individuals), and this function was parameterized by b only (other notations in Eq. 3 are either constants or functions of b). I obtained the maximum-likelihood estimate (mle) of b and used it to find the community-level constants λ_1 and λ_2.

I further analyzed the parameterized METE prediction of the community-level ISD in three ways. First, to compare the parameterized METE prediction with the original METE and other phenomenological models for ISD within each community, I fitted the original METE prediction (with a fixed $b = 2$ from the metabolic theory of ecology), the exponential, the power-law, the two-parameter Weibull, and the three-parameter quasi-Weibull distributions separately to the observed ISD within each tree community. Each of the four phenomenological models was left truncated, and their likelihood functions were taken from Muller-Landau et al. (2006). I compared the parameterized METE model (Eq. 3) with other models using the Akaike information criterion corrected for small sample size (AIC_c) and AIC_c weight. The model with the least AIC_c (or the largest AIC_c weight) was deemed to provide the best fit of ISD for that community. Second, to examine whether sampling variation affects the mle of b, in a given community, I took bootstrap samples (5,000 for each Black Rock Forest plot community and 1,000 for the Barro Colorado Island plot community) of the rescaled dbh of all individuals and repeated the maximum-likelihood estimation for each bootstrap sample. I constructed the 95% bootstrap confidence interval (CI) of b using the 2.5th and 97.5th percentiles of its estimates as the lower and upper confidence bounds, respectively. Third, to evaluate the goodness of fit of the parameterized METE model to the observed ISD for each community, I used the inverse transform sampling (Devroye 1986) to generate independent samples (1,000 for each Black Rock Forest plot community and 100 for the Barro Colorado Island plot community) of the theoretical distribution predicted by the parameterized METE, and I compared each generated sample to the observed ISD using the Kolmogorov–Smirnov (KS) test. If the proportion of KS tests that reject the null hypothesis (P value < 0.05) of

identical distribution between observed data and simulated sample yielded a binomial 95% CI greater than 0.05, then the parameterized METE model failed to describe the empirical ISD for that plot. The same analysis was done for the original METE model and each phenomenological model.

For each species population with at least 10 ($n \geq 10$, for the Black Rock Forest data) or 100 ($n \geq 100$, for the Barro Colorado Island data) individuals, I substituted λ_2 from the corresponding community-level analysis into Eq. 4 and obtained the mle of the intraspecific b. I then repeated the community-level analysis for each population. Specifically, I compared the predictive power of the parameterized METE model, the original METE model, and four phenomenological models (exponential, power law, Weibull, and quasi-Weibull) using AICc and AICc weight. I constructed the 95% bootstrap CI of b using bootstrap samples of each empirical population. Finally, I used the KS test to evaluate the goodness of fit of the parameterized METE model to the observed ISD. The number of bootstrap or random samples used in the last two steps was 1,000 for each species population in the Black Rock Forest data and 100 for each species population in the Barro Colorado Island data.

Quantifying variation in b

I used statistical models and computer simulation to study whether and how ecological variables (e.g., species richness, abundance, and spatial scale) influence b under the parameterized METE framework. The models and simulation were applied to the Black Rock Forest data. First, I used mixed-effects models to study the variation of b across plots, spatial scales (plot vs. subplot) and species at the population level. Second, I used a simulation model and the parameterized METE to analyze the effects of N_0 (total number of individuals in a community), S_0 (number of species in a community), and n (number of conspecific individuals in a population) on b across the hypothetical communities or populations.

I applied linear mixed-effects models to analyze the variation of intraspecific b among populations. The parameterized METE prediction of intraspecific b derived from Eq. 4 was used as the response variable in each mixed-effects model. Plot and species were chosen as random effects, because only limited levels of each variable were observable in the study area. Because a given population was from a plot (oak species) or a central subplot (non-oak species), I assigned each population the corresponding spatial scale (P for plot and SP for central subplot) as a fixed effect in the mixed-effects model to study its effect on b. Furthermore, I treated the population abundance (number of individuals of a given population) as a fixed effect to study the effect of density dependence on b. The combined fixed- and random-effects structure led to 15 mixed-effects models: four types of fixed effects (none, scale only, abundance only, and scale and abundance) paired with four types of random (intercept) effects (none, plot only, species only, and plot and species), excluding the constant model without any fixed or random effect. I fitted each of the 15 mixed-effects models using the maximum-likelihood method and compared their AIC_c weights. I refitted those models with at least 5% AIC_c weight using the restricted maximum-likelihood method for interpretation. I did not use model averaging for these mixed-effects models, because the goal was to study the effect of various biotic and abiotic variables on b, not to come up with the best model for prediction.

I analyzed the dependence of b on the abundance and species richness across communities and populations using a simulation model and the parameterized METE formulas (Eqs. 3 and 4). Details and results of this simulation model are given in Appendix S1.

All analyses were done in R 3.6.0 (R Development Core Team 2019), including the *nleqslv* package (v3.3.2; Hasselman 2018) for solving nonlinear equations and the *sads* package (v0.4.2; Prado et al. 2018) for fitting the species abundance distribution models (see Appendix S1), and the *optim* function for the maximum-likelihood estimation. Random samples of the parameterized METE models were generated using the *samplepdf* function written by W. D. Brinda (2012). R code and description are in Data S1: Rcode and Metadata S1 online.

Results

For the Black Rock Forest data, the parameterized METE model (Eq. 3) yielded the lowest AIC_c when fitted to the observed community-level ISD in 7 of the 12 central subplot communities (Table 1). The mle of the metabolic scaling exponent b of the parameterized METE model ranged from 1.08 to 1.75. The 95% bootstrap CI of b included two in four communities (central subplots of plots A1, A3, C1, and C3) and was lower than two in the other eight communities. In the five communities where the parameterized METE did not give the best fit, the exponential distribution and the quasi-Weibull distribution yielded the lowest AIC_c in two and three communities, respectively. The average AIC_c weights per community were 51% for the parameterized METE model, 3% for the original METE model, 14% for the exponential distribution, 1% for the power-law distribution, 12% for the Weibull distribution, and 19% for the quasi-Weibull distribution. The parameterized METE model provided a reasonable visual description of the cumulative distribution of rescaled dbh in each community (Fig. 1). The proportion of significant KS tests was not greater than 0.05 in any community for random samples of the parameterized METE model and of the quasi-Weibull distribution (Appendix S1: Table S2). The proportion of significant KS tests was greater than 0.05 in 8, 8, 10, and 1 community, respectively, for the original METE model, exponential,

power-law, and Weibull distributions. When fitted to the ISD for the 47 species populations separately, the parameterized METE model (Eq. 4) yielded the lowest AIC_c for 12 populations (Appendix S1: Table S3). The mle of intraspecific b showed large variation, ranging from 0.33 to 6.07 with a median of 1.39 (Fig. 2a; Appendix S1: Figs. S1–S12, Table 2). The 95% bootstrap CI of b included 2 in 14 populations and was lower than or greater than 2 in 23 or 10 populations, respectively. The exponential, power-law, Weibull, and quasi-Weibull distributions yielded the lowest AIC_c for 12, 3, 11, and 10 populations, respectively (Appendix S1: Table S3). The average AIC_c weights per population were 18% for the parameterized METE model, 2% for the original METE model, 19% for the exponential distribution, 7% for the power-law distribution, 27% for the Weibull distribution, and 27% for the quasi-Weibull distribution. The proportion of significant KS tests for the parameterized METE was higher than 0.05 in 26 populations (Appendix S1: Table S4).

For the Barro Colorado Island data, when fitted to the ISD for the entire 50-hectare plot community, the parameterized METE model (Eq. 3) yielded an AIC_c (1,046,152) lower than that of the original METE model (1,083,102), the exponential distribution (1,139,441), and the power-law distribution (1,058,879), and higher than those of the Weibull distribution (1,040,757) and the quasi-Weibull distribution (1,043,011). The mle of b from the parameterized METE model was 1.70, with a 95% bootstrap CI (1.69, 1.71). KS tests showed that all random samples of the parameterized METE model differed from the observed ISD. The results for each of the 1,250 quadrat communities are presented in Appendix S1. For the 160 species with at least 100 individuals each, the parameterized METE model (Eq. 4) yielded the lowest AIC_c for one species population (*Talisia nervosa*), whereas the exponential, power-law, Weibull, and quasi-Weibull distributions yielded the lowest AIC_c for, respectively, 11, 8, 95, and 45 species populations (Appendix S1: Table S5). The mle of b from the parameterized METE model ranged from 0.49 to 8.83, with a median of 1.81 (Fig. 2b). The 95% bootstrap CI of b contained two for 20 species populations, and was less than or greater than two for 84 and 56 species populations, respectively (Appendix S1: Table S6). The proportion of significant KS tests for the parameterized METE was higher than 0.05 in all but one (*Virola surinamensis*) of the 160 species populations (Appendix S1: Table S7). Graphical display of the model fit of the cumulative distribution of rescaled dbh corroborated the statistical finding (Fig. 3, Appendix S1: Figs. S13–S34).

Of the 15 mixed-effects models, those with population abundance as a fixed effect had lower AIC_c than others (Appendix S1: Table S8). The model with both scale and abundance as the fixed effects and no random effect showed the highest AIC_c weight (29.9%). Of the six models with at least 5% AIC_c weight, two contained no random effect and four had either species or plot as the random effect. All six models, after being refitted using the restricted maximum-likelihood method, showed that population abundance had a significantly negative effect on b (P-value < 0.05). The standard

Table 1. Community-level data summary and individual size distribution (ISD) model fitting using the diameter at breast height (dbh) data from the Black Rock Forest.

					AIC_c (AIC_c weight)					
Plot	N_0	S_0	dbh (cm)	b	Parameterized METE (%)	METE (%)	Exponential (%)	Power law (%)	Weibull (%)	Quasi-Weibull (%)
A1	66	11	2.7–60.8	1.65 (1.32, 2.08)	**296.30 (68.6)**	299.62 (13.0)	301.09 (6.2)	317.29 (0.0)	300.30 (9.3)	302.65 (2.9)
A2	121	11	2.4–76.6	1.21 (0.98, 1.49)	**457.38 (90.2)**	539.28 (0.0)	525.26 (0.0)	464.20 (3.0)	463.14 (5.1)	465.30 (1.7)
A3	89	8	2.5–58.4	1.75 (1.44, 2.04)	475.45 (1.5)	476.54 (0.8)	**468.17 (55.4)**	510.73 (0.0)	469.84 (24.0)	470.39 (18.3)
A4	56	8	2.5–54.5	1.58 (1.27, 1.97)	**278.34 (75.3)**	283.38 (6.1)	283.17 (6.7)	299.53 (0.0)	282.56 (9.1)	284.89 (2.9)
B1	84	13	2.4–57.1	1.45 (1.16, 1.96)	**327.78 (90.6)**	346.81 (0.0)	347.93 (0.0)	340.58 (0.2)	332.80 (7.4)	335.51 (1.9)
B2	88	10	2.4–65.1	1.33 (1.08, 1.65)	**390.68 (86.4)**	423.93 (0.0)	415.86 (0.0)	403.00 (0.2)	394.96 (10.2)	397.25 (3.2)
B3	61	9	2.4–56.1	1.14 (0.88, 1.38)	350.55 (3.7)	378.47 (0.0)	352.09 (1.7)	359.23 (0.0)	346.67 (26.0)	**344.73 (68.5)**
B4	104	5	2.5–58.2	1.67 (1.28, 1.99)	**463.58 (96.9)**	471.06 (2.3)	478.22 (0.1)	505.78 (0.0)	475.17 (0.3)	474.34 (0.4)
C1	32	7	2.7–60.2	1.73 (1.26, 2.21)	198.93 (4.4)	197.91 (7.3)	195.66 (22.6)	222.09 (0.0)	197.37 (9.6)	**193.85 (56.0)**
C2	19	4	3.2–64.6	1.08 (0.59, 1.62)	110.56 (11.9)	117.97 (0.3)	109.58 (19.3)	114.09 (2.0)	110.78 (10.6)	**107.45 (55.9)**
C3	32	7	3.6–67.3	1.68 (1.03, 2.51)	166.51 (6.1)	165.60 (9.7)	**161.96 (59.7)**	177.70 (0.0)	164.22 (19.2)	166.83 (5.2)
C4	73	8	2.5–44.3	1.29 (1.04, 1.53)	**312.56 (76.2)**	337.84 (0.0)	329.22 (0.0)	320.87 (1.2)	315.64 (16.3)	317.55 (6.3)

Notes: AIC_c = Akaike's information criterion, corrected; METE = maximum entropy theory of ecology. The "plot" indicates the plot where a central subplot community resides, with N_0 as the total number of individuals and S_0 as the number of species within the community. The range of an individual's dbh (in centimeters) within each community is listed under the "dbh (cm)" column. The maximum-likelihood estimate of the metabolic scaling exponent from the community-level parameterized METE model (Eq. 3) is shown under column "b," with the point estimate obtained from the observed data and the 2.5th and 97.5th percentiles (in parentheses) obtained from 5,000 bootstrap samples within each community. For each community, the AIC_c and AIC_c weights of the parameterized METE model, the original METE model, and the four phenomenological models (exponential, power law, Weibull, and quasi-Weibull) are provided, with boldface indicating the models with the best fit, as measured by the lowest AIC_c (or highest AIC_c weight).

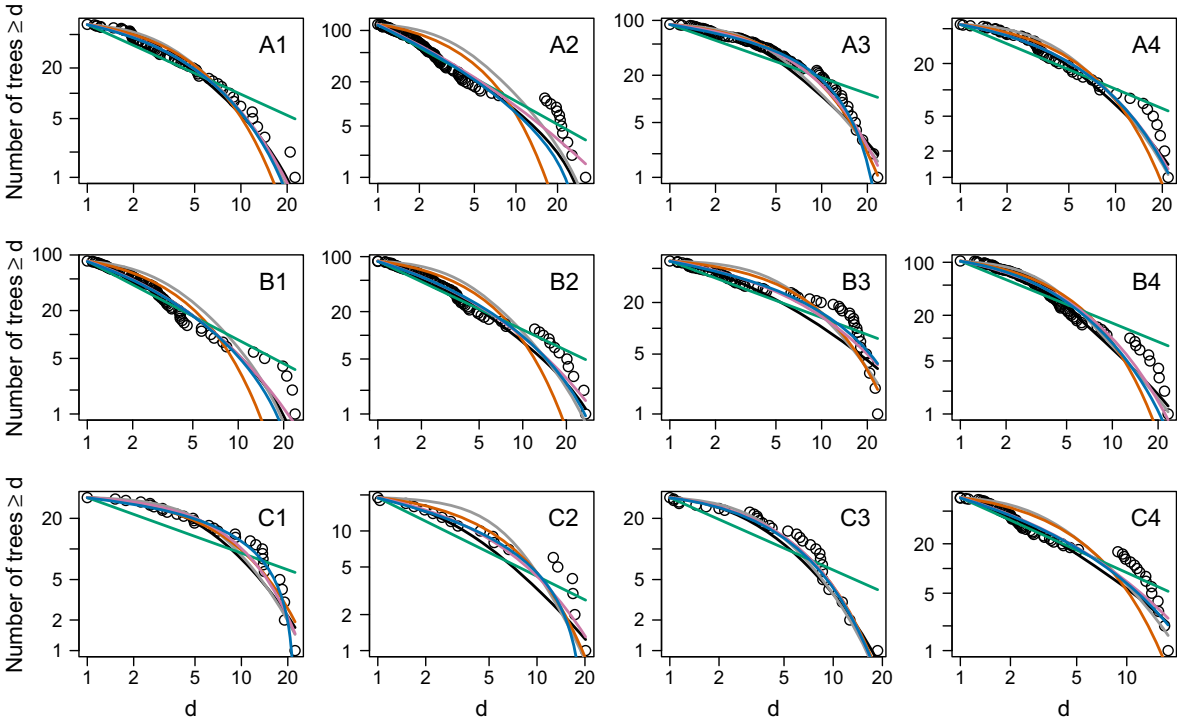

FIG. 1. Number of trees (regardless of species) greater than or equal to d (diameter at breast height [dbh] rescaled by minimum dbh) against d in each central subplot community of the Black Rock Forest. The open circles are observed data. The curves represent the fitted community-level parameterized METE model (Eq. 3, in black), the original METE model (gray), and phenomenological models: exponential (orange), power law (cyan), Weibull (pink), and quasi-Weibull (blue) using the maximum-likelihood method. The name of a plot within which a central subplot community resides is shown at the top right corner of each panel.

deviation of the random effect from the four models with at least 5% AIC_c weight was much higher when the plot rather than the species was used as a random effect.

DISCUSSION

This work provides a novel application of the maximum entropy theory of ecology (METE) in estimating the metabolic scaling exponent (b). The maximum-likelihood approach, which has been shown to provide a reliable estimate of the individual size distribution (ISD) without data binning (Edwards et al. 2017), produces the most empirically plausible estimates of b under the METE framework. Furthermore, the parameterized METE models allow estimation of b at the population and community levels in the absence of direct metabolic rate measurements, which are difficult to obtain from field data. These methodological and practical advantages suggest the parameterized METE as an alternative method of estimating b compared to the traditional regression approaches (Duncan et al. 2007, Sieg et al. 2009, Clarke et al. 2010). However, as an ecological theory, what insights can the parameterized METE models bring to the mechanism of metabolic scaling?

Before answering this question, we need to understand first the descriptive power of the parameterized METE for the community- and population-level ISD studied here. For the tree communities in the central subplots of the Black Rock Forest (in New York, USA) and in the quadrats of the Barro Colorado Island (in central Panama), the parameterized METE model (Eq. 3) showed clear advantages over the original METE model and other phenomenological models when fitted to the empirical ISD (Table 1, Appendix S1: Fig. S35). Because b is the only free parameter in my parameterized METE model, this result suggests that metabolic scaling of individual organisms may contain crucial information that regulates the size distribution at higher levels of biological organization. On the other hand, b estimated from Eq. 3 was less than two in most communities (Table 1, Appendix S1: Fig. S36), which differs from the prediction of the metabolic theory of ecology ($b = 2$, West et al. 1999). Using the Gentry transect data, Enquist and Niklas (2001) showed that the number of individuals (N) scales as a power of the average dbh per individual across communities with an exponent of minus two. If the results by Enquist and Niklas hold for the tree communities in the current study, then the total resource supply (R, measured by total metabolic rate) is a negative power function of the average dbh per individual ($\overline{\text{dbh}}$): $R \propto N\bar{e} \propto (\overline{\text{dbh}})^{-2}(\overline{\text{dbh}})^{b} = (\overline{\text{dbh}})^{b-2}$ with $b-2 < 0$. Here $\bar{e}$ is the average resource use (or metabolic rate) per individual. This indicates that the total resource supply is not independent of the individual size (as

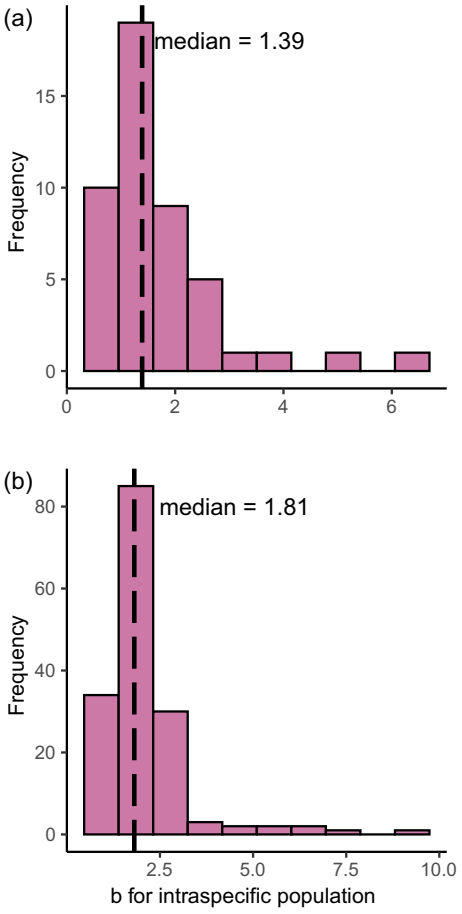

FIG. 2. Histogram of the maximum-likelihood estimate of metabolic scaling exponent (b) for each intraspecific population using the population-level parameterized METE model (Eq. 4), using (a) 47 species populations (with at least 10 individuals each) from the Black Rock Forest and (b) 160 species populations (with at least 100 individuals each) from the Barro Colorado Island. Black dashed lines show the medians of the estimated b.

found in Enquist et al. 1998), which violates the energy equivalence rule (White et al. 2007*a*, *b*). Instead, this implies that communities with smaller individuals will require more resource supply. However, this derivation holds only when the power function evaluated at the average is a good first-order approximation of the average of the power function (see Jensen's inequality in White et al. 2007a, *b* and Bolnick et al. 2011), so that $e \propto \text{dbh}^b$ implies $\bar{e} \propto \text{dbh}^b \approx (\overline{\text{dbh}})^b$.

My parameterized METE models showed variation in b across tree populations and across tree communities. If the allometric scaling between body mass (m) and dbh for plants was $m \propto \text{dbh}^{8/3}$ (West et al. 1999), my community-level analysis showed that the exponent of metabolic scaling with body mass ranges from 0.41 to 0.65 for the Black Rock Forest central subplots and from 0.28 to 0.52 for the Barro Colorado Island quadrats (using the 2.5th and 97.5th percentiles of estimated b [Table 1; Appendix S1: Table S9] multiplied by 3/8), lower than 2/3 (≈ 0.67) and 3/4 ($= 0.75$) from respective evidence (Dodds et al. 2001, White and Seymour 2003, Savage et al. 2004*b*). Hence, the mass-specific metabolic rate (e/m) decreases at a faster speed with the body mass than what the metabolic theory of ecology has predicted (i.e., $e/m \propto m^{-1/4}$). This rate of decrease implies that the contrast between small and large organisms in their rates of mass-specific growth is even greater than that shown with the previous theoretical prediction. My population-level analysis showed a wide range of metabolic scaling exponent with body mass (0.13–1.86 for the Black Rock Forest populations and 0.32–2.02 for the Barro Colorado Island populations, following the above calculations). However, this finding is compromised by the poor fit of the parameterized METE model to the observed population-level ISD (Appendix S1: Tables S3 and S5) and the relatively small number of individuals of species populations (especially for the Black Rock Forest data). Overall, the large variation of b across populations and communities may be attributed to the constraint-based nature of the METE without relying on system-specific mechanisms, or this variation may be explained intrinsically by the ecological variables within the METE formulations. A better understanding of the implication of the parameterized METE models on metabolic scaling requires the development of a theoretical prediction of the mass-dbh allometric scaling within the METE framework (instead of borrowing the scaling relationship from other theories, such as $m \propto \text{dbh}^{8/3}$ in the metabolic theory of ecology; West et al. 1999) and its testing with the same data and statistical methods.

Based on results from the simulation model (Appendix S1: Fig. S37), the asymptotic behavior of b suggests that predictions of the parameterized METE models may follow a central-limit-like theorem in ecologically rich (large S_0) and abundant (large N_0) communities. On the other hand, the positive relation between b and N_0 may imply that the energy acquisition efficiency (as reflected by b) increases as more individuals join the community, but the speed of increase drops as the community continues to include new members and before a saturated stage of energy use is reached. The population-level simulation confirmed the wide range of b (as shown by the empirical analysis) and illustrated the negative relationship between b and the number of individuals within a species (n; Appendix S1: Fig. S38). This means that the energy-acquisition efficiency of conspecific individuals may be constrained by species-specific resource limitations or interspecific competition. The contrast in the effect of abundance on b between the community and the population suggests different metabolic mechanisms are at play.

Several aspects of this work deserve further investigation. First, the data used in my analysis are relatively limited in the spatial scale (about six hectares in the Black Rock Forest plots and 50 hectares in

TABLE 2. Intraspecific b estimated from the population-level parameterized maximum entropy theory of ecology (METE) model (Eq. 4) for individual size distribution using the diameter at breast height data from the Black Rock Forest.

	b								
Plot	BB	BE	BG	BO	CO	RM	RO	SM	WO
A1			1.40 (1.24, 2.08)				2.11 (1.99, 2.78)	**1.27 (1.15, 1.76)**	**6.07 (5.18, 9.89)**
A2	**1.10 (0.98, 1.36)**		**1.42 (1.24, 1.88)**		**0.87 (0.82, 1.31)**	1.54 (1.31, 2.12)	**1.10 (1.04, 1.95)**	1.73 (1.38, 3.60)	**1.25 (1.12, 1.66)**
A3	**2.51 (2.31, 4.02)**	**1.39 (1.25, 1.80)**		**3.33 (3.09, 6.67)**	2.08 (1.97, 2.73)		**2.11 (2.01, 4.27)**		
A4			1.52 (1.38, 2.06)		**0.81 (0.79, 1.76)**	2.03 (1.79, 3.65)	**0.72 (0.70, 1.08)**		
B1	**1.35 (1.21, 1.76)**		**1.45 (1.32, 1.91)**	**3.95 (3.19, 8.90)**	**0.96 (0.88, 1.91)**	1.64 (1.34, 2.75)	1.07 (1.03, 3.85)	1.10 (0.91, 2.40)	
B2			**1.07 (0.95, 1.28)**			**2.37 (2.13, 3.03)**	**1.30 (1.23, 1.73)**	1.71 (1.41, 3.59)	0.98 (0.94, 4.83)
B3					**0.75 (0.71, 1.07)**	2.09 (1.76, 3.03)	**0.43 (0.42, 0.97)**		
B4	**2.30 (2.07, 2.90)**				**0.74 (0.71, 0.79)**	**2.29 (2.13, 3.11)**	**0.88 (0.83, 0.99)**		
C1							**2.28 (2.14, 3.86)**	1.60 (1.45, 2.65)	
C2							**0.83 (0.79, 1.56)**		
C3					**5.13 (4.43, 10.00)**		**1.26 (1.19, 1.57)**		
C4					**0.34 (0.32, 0.39)**	**1.35 (1.16, 1.81)**	**0.33 (0.31, 0.40)**		

Notes: BB = black birch, *Betula lenta*; BE = American beech, *Fagus grandifolia*; BG = black gum, *Nyssa sylvatica*; BO = black oak, *Quercus velutina*; CO = chestnut oak, *Quercus prinus*; RM = red maple, *Acer rubrum*; RO = red oak, *Quercus rubra*; SM = sugar maple, *Acer saccharum*; WO = white oak, *Quercus alba.* The "plot" shows the name of a plot where a species is found. Point estimates are obtained from the observed data and interval estimates are obtained from 1,000 bootstrap samples of each intraspecific population (per plot–species pair). The lower bound and upper bound in each interval are, respectively, the 2.5th percentile and 97.5th percentile of the predicted b using the 1,000 bootstrap samples. Blank cells indicate that a species has fewer than 10 individuals in the corresponding plot or subplot, and the parameterized METE model was not fitted for that species. Boldface indicates that the point estimate is significantly different from two (when the interval estimate does not include two), which is the predicted value from the metabolic theory of ecology (see Introduction).

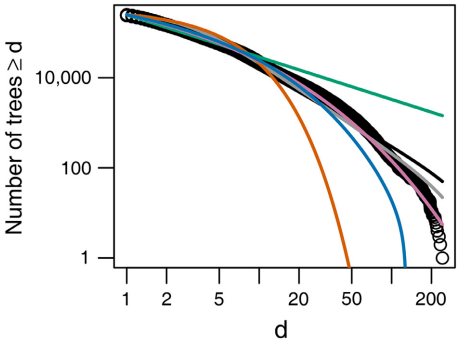

FIG. 3. Number of trees (regardless of species) greater than or equal to d (diameter at breast height [dbh] rescaled by minimum dbh) against d in the whole 50-ha plot community of the Barro Colorado Island. Open circles and curves are defined in the legend of Fig. 1.

the Barro Colorado Island plot) and taxonomic coverage (approximately 300 tree species in total from both data sets). Future studies are needed to evaluate whether the parameterized METE models can be applied to other taxonomic groups (e.g., small mammal box trapping; Kao et al. 2012) at large spatial scales (e.g., forest inventory and analysis; Burrill et al. 2018). Second, the Black Rock Forest has experienced heavy deer browsing over past decades (Schuster et al. 2008), which plays a major role in preventing the oak saplings from growing to their full potential sizes (see gaps of d in Fig. 1). Previous study has shown that the METE provides a better fit to data from undisturbed plots than to data from heavily disturbed plots (Newman et al. 2020). Whether the parameterized METE predictions are affected by human disturbances and the implications of these effects on b are unknown. Large-scale data with various disturbance levels can provide useful insights in this aspect. Third, my parameterized METE models assume that individual metabolic rate scales as a power function of diameter independently of the temperature. The effect of temperature on the metabolic rate has been documented for a wide range of taxa (Gillooly et al. 2001). Although the temperature dependence can be treated as negligible in the tree data used here (data were collected during a single season from the same area), it will play an important role when analyzing data collected from various

temporal and spatial scales. A possible resolution would be to add temperature as a new state variable in the METE formulation. Fourth, related to the third point, it would be interesting to test how other high-order nonlinear scaling relationships between metabolic rate and size (with or without temperature effect; see Kolokotrones et al. 2010) influence the performance and predictions of the parameterized METE models. Finally, in the maximum-likelihood estimation, I assume that the interspecific and intraspecific individuals are identical and independent. Whether such assumptions can be confirmed empirically, and how individual variation impacts the parameterized METE predictions, will need further investigation.

To conclude, my parameterized METE models predicted large variations in b across tree communities and populations. This corroborates previous studies on metabolic scaling (Bokma 2004, White et al. 2005, Glazier 2006, White et al. 2007a, b). Moreover, the parameterized METE allows us to explore theoretical connections between b and ecological variables above the individual level (i.e., S_0, N_0, and n). My findings imply that these ecological variables may act as controlling agents for the energy demand and supply in communities or populations, while constraining the metabolic scaling of organism at the individual level. Such a top-down approach differs from the existing physical models of metabolic scaling that are based on the internal physiological and biological structure of individual organisms (Agutter and Wheatley 2004, Glazier 2005, 2010).

The unique feature of METE in integrating metabolic energy, abundance, and species richness into the same theoretical framework is significant. This feature gives us the opportunity to understand the regularity in nature (e.g., scaling laws) through ecologically fundamental metrics. Although METE has already been used to study numerous ecological scaling patterns and relationships (White et al. 2012, McGlinn et al. 2013, 2015, Xiao et al. 2015), I believe that the door connecting METE and other constraint-based approaches to macroecology has just been opened. For example, Harte and his colleagues have been working on extending the original METE to higher taxonomic levels and to a dynamic model (Harte 2011, Harte and Newman 2014, Harte et al. 2015). O'Dwyer et al. (2017) designed a novel application of mechanistic models to select the constraint variables of METE, which has been debated (Favretti 2017, 2018, Harte 2018). In addition to these theoretical advances, the integration of multiple ecological patterns predicted from METE and the usefulness of METE in quantifying variance across different levels of biological organization deserve more research attention. Finally, whether the ecological variables used in the METE formulation govern metabolic scaling or are by-products of other biological mechanisms that explain the metabolic scaling pattern remains to be seen (McGill 2010). Successful predictions of empirical patterns should not be the only goal and use of constraint-based modeling but, instead, should be the first step toward facilitating a mechanistic understanding of living systems (Bertram et al. 2019).

Acknowledgments

The author thanks William S. F. Schuster for sharing the Black Rock Forest data. The Barro Colorado Island forest dynamics research project was founded by S. P. Hubbell and R. B. Foster, and is now managed by R. Condit, S. Lao, and R. Perez under the Center for Tropical Forest Science and the Smithsonian Tropical Research in Panama. Numerous organizations have provided funding to the Barro Colorado Island research project, principally the U.S. National Science Foundation, and hundreds of field workers have contributed. Matthew Aiello-Lammens, John Harte, Duncan Menge, and H. Brian Underwood provided useful feedback and comments on the preliminary analysis of this work.

Literature Cited

Agutter, P. S., and D. N. Wheatley. 2004. Metabolic scaling: consensus or controversy? Theoretical Biology and Medical Modelling 1:13.

Allen, A. P., J. H. Brown, and J. F. Gillooly. 2002. Global biodiversity, biochemical kinetics, and the energetic-equivalence rule. Science 297:1545–1548.

Bennett, P. M., and P. H. Harvey. 1987. Active and resting metabolism in birds: allometry, phylogeny and ecology. Journal of Zoology 213:327–344.

Bertram, J. 2015. Entropy-related principles for non-equilibrium systems: theoretical foundations and applications to ecology and fluid dynamics. Dissertation. Australian National University, Canberra, Australia.

Bertram, J., E. A. Newman, and R. C. Dewar. 2019. Comparison of two maximum entropy models highlights the metabolic structure of metacommunities as a key determinant of local community assembly. Ecological Modelling 407:108720.

Biro, P. A., and J. A. Stamps. 2010. Do consistent individual differences in metabolic rate promote consistent individual differences in behavior? Trends in Ecology & Evolution 25:653–659.

Bokma, F. 2004. Evidence against universal metabolic allometry. Functional Ecology 18:184–187.

Bolnick, D. I., P. Amarasekare, M. S. Araújo, R. Bürger, J. M. Levine, M. Novak, V. H. W. Rudolf, S. J. Schreiber, M. C. Urban, and D. A. Vasseur. 2011. Why intraspecific trait variation matters in community ecology. Trends in Ecology & Evolution 26:183–192.

Brinda, W. D. 2004. Sampling from an arbitrary density. http://blog.quantitations.com/tutorial/2012/11/20/sampling-from-anarbitrary-density

Brown, J. H., J. F. Gillooly, A. P. Allen, V. M. Savage, and G. B. West. 2004. Toward a metabolic theory of ecology. Ecology 85:1771–1789.

Brummer, A., and E. Newman. 2019. Derivations of the core functions of the maximum entropy theory of ecology. Entropy 21:712.

Burrill, E., A. M. Wilson, J. A. Turner, S. A. Pugh, J. Menlove, G. Christiansen, B. L. Conkling, and W. David. 2018. The forest inventory and analysis database: Database description and user guide version 8.0 for phase 2. U.S. Department of Agriculture, Forest Service, Washington, D.C., USA.

Clarke, A., P. Rothery, and N. J. Isaac. 2010. Scaling of basal metabolic rate with body mass and temperature in mammals. Journal of Animal Ecology 79:610–619.

Cohen, J. E., M. Xu, and W. S. F. Schuster. 2012. Allometric scaling of population variance with mean body size is predicted from Taylor's law and density–mass allometry. Proceedings of the National Academy of Sciences of the United States of America 109:15829–15834.

Condit, R. 1998. Tropical forest census plots: methods and results from Barro Colorado Island, Panama and a comparison with other plots. Springer Science & Business Media, Berlin, Germany.

Condit, R., R. Pérez, S. Aguilar, S. Lao, R. Foster, and S. Hubbell. 2019*a*. Complete data from the Barro Colorado 50-ha plot: 423617 trees, 35 years, v3. DataONE, dataset 2019. http://doi.org/10.15146/5xcp-0d46

Condit, R., R. Pérez, S. Aguilar, S. Lao, R. Foster, and S. Hubbell. 2019*b*. BCI 50-ha plot taxonomy, v4. DataONE, data set 2019. https://doi.org/10.15146/R3FH61

Damuth, J. 1981. Population density and body size in mammals. Nature 290:699–700.

Devroye, L.1986. Non-uniform random variate generation. Springer, New York, New York, USA.

Dodds, P. S., D. H. Rothman, and J. S. Weitz. 2001. Re-examination of the "3/4-law" of metabolism. Journal of Theoretical Biology 209:9–27.

Duncan, R. P., D. M. Forsyth, and J. Hone. 2007. Testing the metabolic theory of ecology: allometric scaling exponents in mammals. Ecology 88:324–333.

Edwards, A. M., J. P. Robinson, M. J. Plank, J. K. Baum, and J. L. Blanchard. 2017. Testing and recommending methods for fitting size spectra to data. Methods in Ecology and Evolution 8:57–67.

Enquist, B. J., J. H. Brown, and G. B. West. 1998. Allometric scaling of plant energetics and population density. Nature 395:163–165.

Enquist, B. J., and K. J. Niklas. 2001. Invariant scaling relations across tree-dominated communities. Nature 410:655–660.

Favretti, M. 2017. Remarks on the maximum entropy principle with application to the maximum entropy theory of ecology. Entropy 20:11.

Favretti, M. 2018. Maximum entropy theory of ecology: a reply to Harte. Entropy 20:308.

Gillooly, J. F., J. H. Brown, G. B. West, V. M. Savage, and E. L. Charnov. 2001. Effects of size and temperature on metabolic rate. Science 293:2248–2251.

Glazier, D. S. 2005. Beyond the '3/4-power law': variation in the intra- and interspecific scaling of metabolic rate in animals. Biological Reviews 80:611–662.

Glazier, D. S. 2006. The 3/4-power law is not universal: evolution of isometric, ontogenetic metabolic scaling in pelagic animals. BioScience 56:325–332.

Glazier, D. S. 2010. A unifying explanation for diverse metabolic scaling in animals and plants. Biological Reviews 85:111–138.

Harte, J. 2011. Maximum entropy and ecology: a theory of abundance, distribution, and energetics. Oxford University Press, Oxford, UK.

Harte, J. 2018. Maximum entropy and theory construction: a reply to Favretti. Entropy 20:285.

Harte, J., and J. Kitzes. 2015. Inferring regional-scale species diversity from small-plot censuses. PLoS ONE 10:e0117527.

Harte, J., and E. A. Newman. 2014. Maximum information entropy: a foundation for ecological theory. Trends in Ecology and Evolution 29:384–389.

Harte, J., E. A. Newman, and A. J. Rominger. 2017. Metabolic partitioning across individuals in ecological communities. Global Ecology and Biogeography 26:993–997.

Harte, J., A. Rominger, and W. Zhang. 2015. Integrating macroecological metrics and community taxonomic structure. Ecology Letters 18:1068–1077.

Harte, J., A. B. Smith, and D. Storch. 2009. Biodiversity scales from plots to biomes with a universal species–area curve. Ecology Letters 12:789–797.

Harte, J., T. Zillio, E. Conlisk, and A. B. Smith. 2008. Maximum entropy and the state-variable approach to macroecology. Ecology 89:2700–2711.

Hasselman, B.2018. nleqslv: solve systems of nonlinear equations. R package version 3.3.2. https://CRAN.R-project.org/package=nleqslv

Hemmingsen, A. M. 1960. Energy metabolism as related to body size and respiratory surface, and its evolution. Reports of the Steno Memorial Hospital (Copenhagen) 13:1–110.

Heusner, A. A. 1982. Energy metabolism and body size I. Is the 0.75 mass exponent of Kleiber's equation a statistical artifact? Respiration Physiology 48:1–12.

Hubbell, S. P. 2001. The unified neutral theory of biodiversity and biogeography. Princeton University Press, Princeton, New Jersey, USA.

Hubbell, S. P., R. B. Foster, S. T. O'Brien, K. E. Harms, R. Condit, B. Wechsler, S. J. Wright, and S. Loo de Lao. 1999. Light gap disturbances, recruitment limitation, and tree diversity in a neotropical forest. Science 283:554–557.

Hubbell, S. P., R. Condit, and R. B. Foster.2005. Barro Colorado Forest census plot data. http://ctfs.si.edu/webatlas/datasets/bci

Huxley, J. 1932. Problems of relative growth. Methuen & Co., London, UK.

Isaac, N. J., and C. Carbone. 2010. Why are metabolic scaling exponents so controversial? Quantifying variance and testing hypotheses. Ecology Letters 13:728–735.

Jaynes, E. T. 1957. Information theory and statistical mechanics. Physical Review 106:620–630.

Kao, R. H., et al. 2012. NEON terrestrial field observations: designing continental-scale, standardized sampling. Ecosphere 3:1–17.

Kleiber, M. 1932. Body size and metabolism. Hilgardia 6:315–353.

Kolokotrones, T., V. Savage, E. J. Deeds, and W. Fontana. 2010. Curvature in metabolic scaling. Nature 464:753–756.

McGill, B. J. 2010. Towards a unification of unified theories of biodiversity. Ecology Letters 13:627–642.

McGlinn, D. J., X. Xiao, J. Kitzes, and E. P. White. 2015. Exploring the spatially explicit predictions of the maximum entropy theory of ecology. Global Ecology and Biogeography 24:675–684.

McGlinn, D. J., X. Xiao, and E. P. White. 2013. An empirical evaluation of four variants of a universal species–area relationship. PeerJ 1:e212.

Muller-Landau, H. C., et al. 2006. Comparing tropical forest tree size distributions with the predictions of metabolic ecology and equilibrium models. Ecology Letters 9:589–602.

Nagy, K. A., I. A. Girard, and T. K. Brown. 1999. Energetics of free-ranging mammals, reptiles, and birds. Annual Review of Nutrition 19:247–277.

Newman, E. A., M. E. Harte, N. Lowell, M. Q. Wilber, and J. Harte. 2014. Empirical tests of within- and across-species energetics in a diverse plant community. Ecology 95:2815–2825.

Newman, E. A., M. Q. Wilber, K. E. Kopper, M. A. Moritz, D. A. Falk, D. McKenzie, and J. Harte. 2020. Disturbance macroecology: a comparative study of community structure

metrics in a high-severity disturbance regime. Ecosphere 11: e03022.
O'Dwyer, J. P., A. Rominger, and X. Xiao. 2017. Reinterpreting maximum entropy in ecology: a null hypothesis constrained by ecological mechanism. Ecology Letters 20:832–841.
Patterson, M. R. 1992. A mass transfer explanation of metabolic scaling relations in some aquatic invertebrates and algae. Science 255:1421–1423.
Prado, P. I., M. D. Miranda, and A. Chalom.2018. sads: maximum likelihood models for species abundance distributions. R package version 0.4.2. https://CRAN.R-project.org/package=sads
R Development Core Team. 2019. R: a language and environment for statistical computing. R Foundation for Statistical Computing, Vienna, Austria. https://www.R-project.org/
Reich, P. B., M. G. Tjoelker, J. L. Machado, and J. Oleksyn. 2006. Universal scaling of respiratory metabolism, size and nitrogen in plants. Nature 439:457–461.
Rominger, A. J., and C. Merow. 2017. meteR: an r package for testing the maximum entropy theory of ecology. Methods in Ecology and Evolution 8:241–247.
Rosenfeld, J., T. Van Leeuwen, J. Richards, and D. Allen. 2015. Relationship between growth and standard metabolic rate: measurement artefacts and implications for habitat use and life-history adaptation in salmonids. Journal of Animal Ecology 84:4–20.
Rubner, M. 1883. Ueber den einfluss der korpergrosse auf stoffund kaftwechsel. Zeitschrift fur Biologie 19:535–562.
Russo, S. E., S. K. Robinson, and J. Terborgh. 2003. Size–abundance relationships in an Amazonian bird community: implications for the energetic equivalence rule. American Naturalist 161:267–283.
Savage, V. M., J. F. Gillooly, J. H. Brown, G. B. West, and E. L. Charnov. 2004*a*. Effects of body size and temperature on population growth. American Naturalist 163:429–441.
Savage, V. M., J. F. Gillooly, W. H. Woodruff, G. B. West, A. P. Allen, B. J. Enquist, and J. H. Brown. 2004*b*. The predominance of quarter-power scaling in biology. Functional Ecology 18:257–282.
Schuster, W. S. 2007. Future of Oak Forests experiment—DBH of trees in Black Rock Forest, New York, USA, 2007. Version 1. Environmental data initiative. http://dx.doi.org/https://doi.org/10.6073/pasta/da52f36341eebd575824d9201d0b3f31.
Schuster, W. S., K. L. Griffin, H. Roth, M. H. Turnbull, D. Whitehead, and D. T. Tissue. 2008. Changes in composition, structure and aboveground biomass over seventy-six years (1930–2006) in the Black Rock Forest, Hudson Highlands, southeastern New York State. Tree Physiology 28:537–549.
Sears, M. W. 2005. Resting metabolic expenditure as a potential source of variation in growth rates of the sagebrush lizard. Comparative Biochemistry and Physiology Part A: Molecular & Integrative Physiology 140:171–177.
Shannon, C. E. 1948. A mathematical theory of communication. Bell System Technical Journal 27:379–423.
Sieg, A. E., M. P. O'Connor, J. N. McNair, B. W. Grant, S. J. Agosta, and A. E. Dunham. 2009. Mammalian metabolic allometry: do intraspecific variation, phylogeny, and regression models matter? American Naturalist 174:720–733.
Steyermark, A. C. 2002. A high standard metabolic rate constrains juvenile growth. Zoology 105:147–151.
West, G. B., J. H. Brown, and B. J. Enquist. 1997. A general model for the origin of allometric scaling laws in biology. Science 276:122–126.
West, G. B., J. H. Brown, and B. J. Enquist. 1999. A general model for the structure and allometry of plant vascular systems. Nature 400:664–667.
White, C. R., P. Cassey, and T. M. Blackburn. 2007*a*. Allometric exponents do not support a universal metabolic allometry. Ecology 88:315–323.
White, C. R., N. F. Phillips, and R. S. Seymour. 2005. The scaling and temperature dependence of vertebrate metabolism. Biology Letters 2:125–127.
White, C. R., and R. S. Seymour. 2003. Mammalian basal metabolic rate is proportional to body mass2/3. Proceedings of the National Academy of Sciences of the United States of America 100:4046–4049.
White, C. R., and R. S. Seymour. 2005. Allometric scaling of mammalian metabolism. Journal of Experimental Biology 208:1611–1619.
White, E. P., S. M. Ernest, A. J. Kerkhoff, and B. J. Enquist. 2007*b*. Relationships between body size and abundance in ecology. Trends in Ecology & Evolution 22:323–330.
White, E. P., K. M. Thibault, and X. Xiao. 2012. Characterizing species abundance distributions across taxa and ecosystems using a simple maximum entropy model. Ecology 93:1772–1778.
Xiao, X., D. J. McGlinn, and E. P. White. 2015. A strong test of the maximum entropy theory of ecology. American Naturalist 185:E70–E80.

Supporting Information

Additional supporting information may be found in the online version of this article at http://onlinelibrary.wiley.com/doi/10.1002/ecy.3011/suppinfo